

THE TACQ COMPUTER PROGRAM FOR AUTOMATIC TIME DOMAIN REFLECTOMETRY MEASUREMENTS: II. WAVEFORM INTERPRETATION METHODS¹

Steven R. Evett

ABSTRACT. *Despite the increased use of time domain reflectometry (TDR) for measurement of soil water content and bulk electrical conductivity (BEC), there are few public releases of software for TDR system control. Even though graphical interpretation of the waveform to find pulse travel times is key to success with the method, the few published descriptions of computer methods are incomplete. The TACQ program, under development since the early 1990s on a wide variety of soils, allows control of multiplexed systems supporting up to 256 TDR probes. Waveform interpretation methods are user-controlled and allow interpretation using various methods reported in the literature or methods available only in TACQ. The default methods allow automatic interpretation of waveforms from a variety of media including loose, air-dry soil, and wet clay. The present study shows that interpretation methods can have a large effect on reported water contents. The additive effects can result in water content change errors as large as $0.08 \text{ m}^3 \text{ m}^{-3}$ as the soil wets and dries, and as TDR system temperature changes over a season. Thus, the interpretation methods used should be reported in rigorous studies involving TDR water content determination, calibration, and temperature effects. The TACQ program, and documentation, may be downloaded from (<http://www.cprl.ars.usda.gov/programs/>).*

Keywords. *TDR, Time domain reflectometry, Computer program, Soil water content, Waveform interpretation, Bulk electrical conductivity, BEC.*

Time domain reflectometry (TDR) became known as a useful method for soil water content and bulk electrical conductivity measurement in the 1980s; and automated TDR systems for water content measurement were described by Baker and Allmaras (1990), Heimovaara and Bouten (1990), Herkelrath et al. (1991), and Evett (1993, 1994). Commercial systems became available in the late 1980s. The TDR method relies on graphical interpretation of the waveform reflected from that part of the waveguide that is the probe (Fig. 1). The interpretation yields the travel time, t_r , of an electrical pulse along the rods of the probe; and t_r and probe length are then related to water content. Despite its key importance in the TDR method, only a few papers have been published describing waveform interpretation, notably Topp et al. (1982), Baker and Allmaras (1990), and Heimovaara (1993). The first paper in this series (Evett, 2000) described the TACQ program for controlling an automatic TDR system. It began with a discussion of aspects of the TDR method that influence program design, described program design objectives, and discussed program capabilities

and operation. Because waveform interpretation is a particular difficulty of the TDR method, this paper continues with a discussion of waveform shapes, factors that influence shape, and graphical algorithms for automated waveform interpretation and some errors that can occur.

Baker and Allmaras (1990) described how the first derivative of the waveform could be used to find some of the important features related to travel time of the step pulse. These and other features are illustrated in Figure 1. An example of waveform interpretation for a 20 cm TDR probe in wet sand shows how tangent lines are fitted by TACQ to several waveform features (Fig. 2). Intersections of the tangent lines define times related to (i) the separation of the outer braid from the coaxial cable so that it can be connected to one of the probe rods, $t_{1.bis}$; (ii) the time when the pulse exits the handle and enters the soil, t_1 ; and (iii) the time when the pulse reaches the ends of the probe rods, t_2 .

Graphical interpretation depends on the fact that the probe design itself introduces impedance changes in the waveguide. The impedance, Z (Ω), of a transmission

¹Article has been reviewed and approved for publication by the Information and Electrical Technologies Division of ASAE. Presented as ASAE Paper No. 98-3182. Contribution of the U.S. Department of Agriculture, Agricultural Research Service, Southern Plains Area, Conservation and Production Research Laboratory, Bushland, Texas. Article was submitted for publication in August, 1998; approved for submission by USDA-ARS. This work was done in part under the scope of Cooperative Research and Development Agreement No. 58-3K95-5-405 between USDA-ARS and Dynamax, Inc., Houston, TX, and in part under the USAID funded Agricultural Technology Utilization and Transfer Project. Author is Soil Scientist, Conservation and Production Research Laboratory, 2300 Experiment Station Road, Bushland, TX 79012, U.S.A., e-mail: srevett@cprl.ars.usda.gov (Internet: <http://www.cprl.ars.usda.gov>) This work was prepared by a USDA employee as part of his official duties and cannot legally be copyrighted. The fact that the private publication in which the article appears is itself copyrighted does not affect the material of the U.S. Government, which can be reproduced by the public at will.

line (i.e. waveguide) is

$$Z = Z_0(\epsilon)^{-0.5} \quad (1)$$

where Z_0 is the characteristic impedance of the line (when air fills the space between conductors) and ϵ is the permittivity of the homogeneous medium filling the space between conductors. For a parallel transmission line (the two rods in the soil), the characteristic impedance is a function (Williams, 1991) of the wire diameter, d , and spacing, s (Fig. 1):

$$Z_0 = 120 \ln\{2s/d + [(s/d)^2 - 1]^{0.5}\} \quad (2)$$

or, if $d \ll s$:

$$Z_0 = 120 \ln(2s/d) \quad (3)$$

For a coaxial transmission line the characteristic impedance is:

$$Z_0 = 60 \ln(D/d) \quad (4)$$

where D and d are the diameters of the outer and inner conductors, respectively.

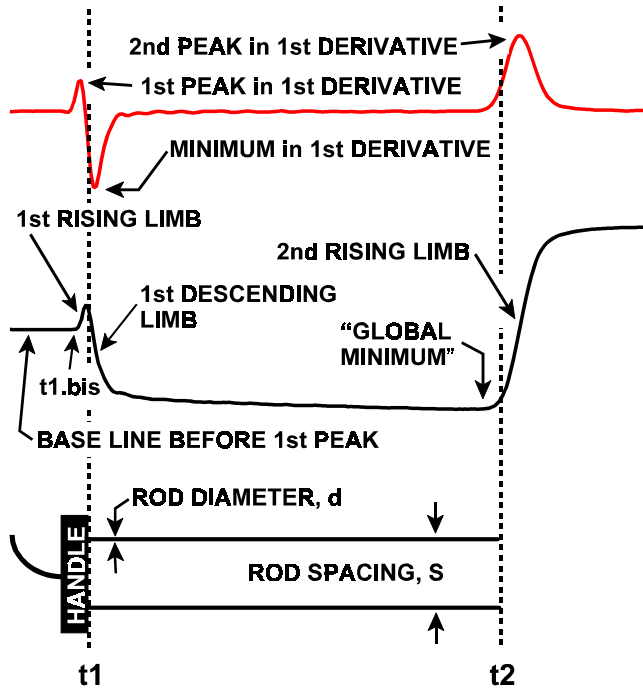


Figure 1. TDR waveform (middle) for a wet sand and its first derivative (top) showing features useful for graphical interpretation and their relationship to a bifilar TDR probe (bottom) with rod spacing, S , and rod diameter, d . The dashed vertical lines indicate times t_1 and t_2 , the difference between which is the travel time, t_t , that is related to water content.

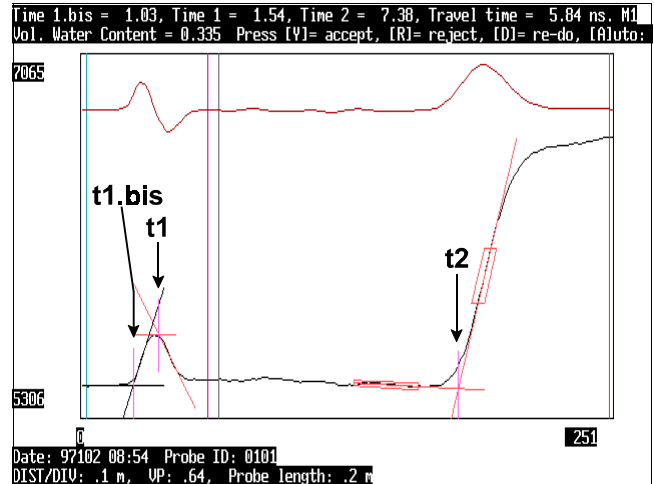


Figure 2. Example from TACQ of graphical interpretation of a waveform from a probe in wet sand. Vertical lines denoting times $t_{1.bis}$, t_1 , and t_2 have been marked by arrows and labels. A horizontal line, drawn tangent to the waveform base line at the far left, intersects with a line drawn tangent to the first rising limb of the waveform to define $t_{1.bis}$. A horizontal line drawn tangent to the peak intersects with a line drawn tangent to the descending waveform after the peak to define t_1 . The water content is calculated from Eq. 7 of Topp et al (1980). The width of the waveform window is 1 m or $1/(0.64 \epsilon_0) = 5.2$ ns. There are 251 data points in the waveform.

From Eqs. 1 through 4 it is apparent that impedance, Z , increases as wire spacing increases, and decreases as ϵ (or water content) increases for any probe type (Fig. 3). In the probe handle, the wire spacing increases from that of the coaxial cable to that of the probe rods. The resulting impedance increase causes the waveform level to rise (first rising limb in Fig. 1). If the porous medium in which the probe rods are embedded is wet, then the permittivity of that medium will be higher than that of the epoxy probe handle. This causes a decrease in impedance, which results in the descent of the reflected waveform level as the step voltage leaves the handle and enters the rods in the soil (first descending limb,

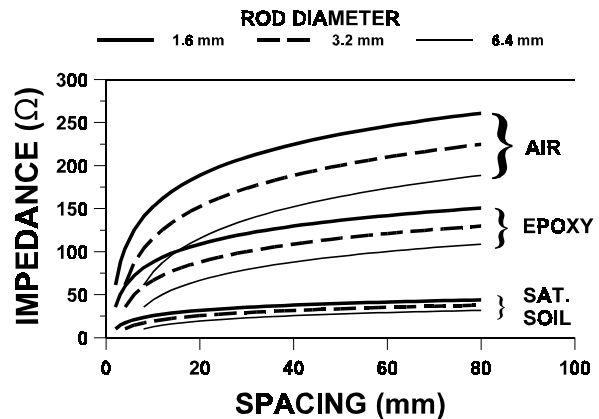


Figure 3. Influence of rod spacing, rod diameter, and permittivity of the medium on impedance of the waveguide according to Eqs. 1 and 2. Permittivities are: AIR, unity; EPOXY, close to 3; and SATurated SOIL, approx. 35.

Fig. 1). The combination of impedance increase at the handle and impedance decrease after the handle gives the peak in the waveform. The rod ends are another impedance change in the waveguide, in this case an open circuit. The remaining energy in the voltage step is reflected back at the rod ends, which represent an impedance increase (second rising limb, Fig. 1). As will be discussed later, waveform shapes different from those shown in Figs. 1 and 2 result from different soil types and conditions (e.g. dry soil, or wet clays). A program for automatic TDR data acquisition must be able to acquire the waveform from the probe and correctly interpret it graphically. It should be able to accomplish this despite different cable lengths to the probes, different probe lengths and rod spacings, and different soil conditions.

The objective of this work was to create a computer program for TDR system control that would correctly interpret waveforms from probes of widely varying length in many different soils and soil conditions to give travel times and water contents automatically.

EARLY WAVEFORM INTERPRETATIONS

Topp et al. (1982) described a method of interpreting waveforms captured on paper using a chart recorder or by photographing an oscilloscope screen. This analysis consisted of two graphical algorithms. Algorithm 1 consisted of drawing a horizontal line across the top of the first peak, and drawing a line tangent to the descending limb of the first peak. The intersection of these lines defined t_1 , as illustrated in Fig. 2. Algorithm 2 consisted of drawing a horizontal line tangent to the base line between the first peak and second inflection, and drawing a line tangent to the second inflection. The intersection of the latter two lines defined t_2 . The voltage step travel time, in the part of the waveguide that was buried in the soil, was $t_t = t_2 - t_1$. Peaks and inflections were identified by eye and no computer code or algorithms were presented.

Baker and Allmaras (1990) discussed a computer program for interpretation of waveforms following the ideas of Topp et al. (1982). The program, which was not published, included the following steps applied to a waveform consisting of 200 data points (Fig. 4):

- 1) Smooth and differentiate the data (Savitsky and Golay, 1964).
- 2) Use a loop to search the waveform data for the global minimum, VMIN, and associated time, $t_{2.1}$.
- 3) Find the local maximum, V1MAX, and associated time, t_{1p} , in the data between the first point and $t_{2.1}$. This is the time, t_{1p} , of the

first peak.

- 4) Find the most negative derivative, DMIN, the corresponding time, t_{DMIN} and waveform value, V_{tDMIN} , in a region of 25 points following t_{1p} . The slope of the first descending limb is DMIN.
- 5) Define a line, with intercept V1MAX and slope of zero, that is horizontal and tangent to the first peak. Define a second line, with slope DMIN and intercept such that it passes through V_{tDMIN} at t_{DMIN} . Solve for the intersection point of the two lines, and the associated time, t_1 , that corresponds to the point where the rods exit the handle.
- 6) Find the maximum derivative, D2MAX, in a region of 25 points following VMIN, and associated time $t_{2.2}$ and waveform value $V_{t2.2}$.
- 7) Define a line tangent to the second inflection with slope D2MAX and passing through $V_{t2.2}$ at $t_{2.2}$. Define a horizontal line tangent to VMIN. Solve for the intersection of these lines to find t_2 , the time corresponding to the ends of the rods.

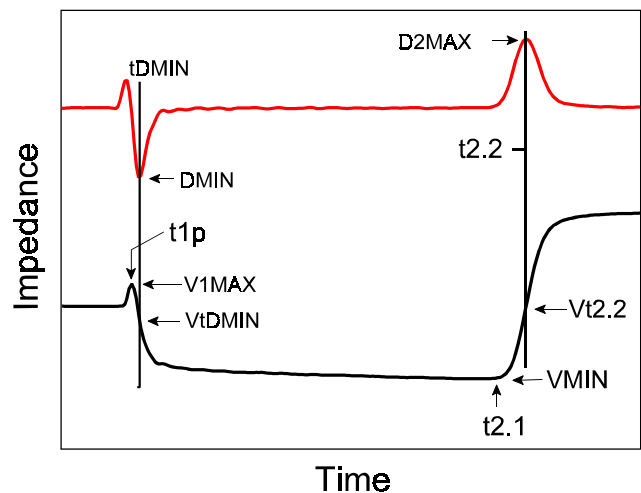


Figure 4. The TDR waveform (bottom) and its first derivative (top) with features identified by Baker and Allmaras (1990) (our nomenclature).

The travel time of the voltage step through the exposed length of the rods was $t_t = t_2 - t_1$. While these algorithms worked well for relatively moist soils, there were problems with the absence of DMIN and absence or movement of VMIN and associated times in waveforms for dry, low bulk density soils.

Heimovaara and Bouten (1990) described a computer program that involved fitting lines to the second inflection and to the base line between t_1 and t_2 . The regions of data points to which these lines were fit

were determined empirically for a given probe. Also, these authors recognized that the waveform might not always descend at t_1 . Because of this, they introduced the concept of fitting lines to the rising limb of the first inflection and to the base line before the first inflection, and using the intersection of these lines to define a time corresponding to the point of separation of the cable conductors. This time is termed $t_{1.bis}$ in this paper, and is illustrated in Fig. 2. A correction time was added to $t_{1.bis}$ to obtain t_1 . This correction time was determined by performing a single measurement in air before probe installation.

FACTORS INFLUENCING WAVEFORM SHAPE

Many conditions may alter the waveform from the classical forms displayed in Figures 1, 2 and 4. Early computer algorithms emphasized finding the minimum, VMIN, and its time, $t_{2.1}$; the second maximum in the first derivative, D2MAX, and its time, $t_{2.2}$; and the minimum of the first derivative, DMIN, and its time, t_{DMIN} (see Fig. 4). In humid environments, where soils are seldom dry, and are well leached so that bulk electrical conductivity is low, these features are found in almost all waveforms and can be reliably used as keys for computer analysis. Also, some of the first field probes consisted of two stainless steel rods connected to 200 Ω twin-lead antenna cable. Because impedance in the soil is almost always less than 200 Ω (Fig. 3), there was always a drop in the waveform at the transition from cable to probe rods. This fact tended to favor the use of the earlier algorithms. However, even for these probes, the position of VMIN may be closer to t_1 than to t_2 in dry soils. Today, most commonly available TDR probes are connected directly to 50 Ω coaxial cable. For these probes in dry soils, DMIN and the descending limb of the first peak may disappear, making t_1 difficult to find. Also, in dry soils, the position of VMIN may change dramatically, moving from the right side to the left side of the waveform between t_1 and t_2 , and causing interpretation problems. In soils with high bulk electrical conductivity, the waveform may rise only slowly at the point corresponding to the ends of the rods; making the value of D2MAX so low as to be lost in the noise level of the first derivative. These and other factors influencing waveform shape are discussed here. Later, algorithms will be presented that allow interpretation of waveforms despite these changes in shape.

INFLUENCE OF PROBE DESIGN ON WAVEFORM SHAPE

The height of the first peak increases with the separation distance of the rods because the impedance at this point in the waveguide increases with the separation distance (Eq. 2; Fig. 3). The impedance and peak height are inversely proportional to the diameter of the rods. The height is also influenced by the permittivity of the material separating the proximal ends of the rods in the handle (Eq. 1). For a handle made of epoxy (ϵ_a approx. 3), rod diameter of 3.2 mm and spacing of 30 mm the characteristic impedance increases from 50 ohms in the cable to 152 ohms in the part of the stainless steel waveguide embedded in the handle (Fig. 3). The pulse travel time between $t_{1.bis}$ and t_1 increases with the permittivity of the material between the point of splitting the antenna cable and the connections to the rods. The pulse travel time also increases with the separation distance of the rods. Finally, this travel time increases with the distance between the split in the cable and the point of connection to the rods.

Consider an early type of TDR probe consisting of two stainless steel rods buried parallel to one another in the soil, with the proximal ends connected to the split ends of a bifilar antenna cable. Connections were sometimes made using alligator clips, sometimes soldered, and were sometimes made by clamping the wire to the rod with a screw. The perpendicular distance between the rods was the separation distance. Typically the antenna cable would have a characteristic impedance of 200 ohms. A balun would usually be used to connect the antenna cable to the cable tester, in order to match impedances (thus lowering signal loss and distortion) between the antenna cable and the 50 ohm waveguide of the cable tester. For this probe, the connections, and some of the split wire, are separated by the soil between the proximal ends of the rods. There is no first peak for this probe, because the waveform always drops from a level corresponding to the 200 Ω cable to a level corresponding to the impedance at the proximal ends of the rods. But, the point at which the waveform drops is influenced by the water content of the intervening soil (assuming the probe is buried). For dry soil the impedance may be nearly the same as for epoxy but for wet soil the value of ϵ_a may approach 35 and the impedance may be 30 ohms or lower (Fig. 3).

Using a probe made with antenna cable and two rods, one can see several reasons why the position of the drop in the waveform and the time of t_1 might not be reproducible between probes in the field. The length of cable split may vary, the separation distance at the

proximal rod ends may vary (over time even if controlled at installation), and the permittivity of the porous medium separating the two wires of the cable may vary in time and space between the cable split and the point of connection to the rods. If the rods are installed vertically, and the point of connection is at the soil surface, the split cable may be separated by air; whereas if the probe is installed deeper in the soil, the split cable will be separated (along at least some of its length) by soil that varies in permittivity as it wets and dries.

For these reasons, the TDR probes commercially available today are invariably made with the split in the cable (usually coaxial cable) and the cable connections to the rods embedded in a material of consistent and constant permittivity. This embedding results in a rigid configuration, usually called the handle (Fig. 1). The handle may be made of epoxy resin, delrin, polymethyl methacrylate (acrylic), RTV silicone or some other plastic and may contain metal for shielding or connection of rods. These handles share the properties of a fixed separation distance, fixed permittivity of the material separating the conductors of the waveguide in the handle (with some minor temperature variations), fixed distance between the cable split and the point of connection to the rods, and fixed distance between the point of connection at the proximal ends of the rods and the point at which the rods exit the handle and enter the soil. Such handles provide optimal conditions for reliable algorithms determining $t_{1.bis}$ and t_1 , and the remaining discussion will assume such a handle.

It has been argued (e.g., Spaans and Baker, 1993), that in order to match impedances (thus lowering signal loss and distortion) between the coaxial cable and the two rods in a bifilar probe, a balun should be used at the point of connection. Also, the balun should serve to convert the unbalanced signal in the coaxial cable (where the inner conductor carries the waveform and the outer conductor remains at virtual ground) to a balanced signal in the two rods (where both conductors carry the waveform). The argument states that if a balun is absent the unbalanced signal will tend to balance as it travels down the rods, eventually becoming closely balanced at some point along the rods. But, between the handle and that point, the signal reflections will be distorted due to the partial imbalance. If the rods are very short, the distorted portion of the waveform may interfere with the second inflection. The trifilar probe responds to this concern by providing a waveguide that is geometrically similar to a coaxial waveguide (Zegelin et al., 1989). Measurements by Zegelin et al. (1989)

showed only minor differences in waveform shape between trifilar and coaxial waveguides.

INFLUENCE OF DRY SOIL ON WAVEFORM SHAPE

As the soil dries, the first descending limb of the waveform (Fig. 1) becomes less steep, and may disappear. Because dry soil has about the same permittivity as the plastic materials used in most probe handles, there may be little or no impedance change between the waveguide in the handle and in the soil. Indeed, if the soil is both dry and of low bulk density, the impedance of the waveguide may actually increase in the soil compared with the handle. Both conditions cause the first descending limb to be almost absent, and may cause the waveform level to rise between t_1 and t_2 (between vertical lines in Fig. 5), so that V_{MIN} is located close to, or before, t_1 . This renders ineffective both algorithm 1 of Topp et al. (1982) and the corresponding methods of Baker and Allmaras (1990). Dry soils of low bulk density are usually found close to the surface. This is where the TDR method enjoys its greatest advantage compared with neutron scattering, its nearest competitor. Thus, it is imperative that the TDR method be usable in such soils. For dry soil, the second inflection, caused by the distal ends of the rods, is invariably steep and high, making it easy to find by searching for $D2MAX$. However, the global minimum may not occur after t_1 , or the position of the local minimum may shift from just before the second inflection to a point just after the first peak, or to any intermediate position (Fig. 5). This causes variations in the intersection of the two lines (horizontal tangent to global minimum and tangent to second inflection) that have no relation to the travel time, t_r .

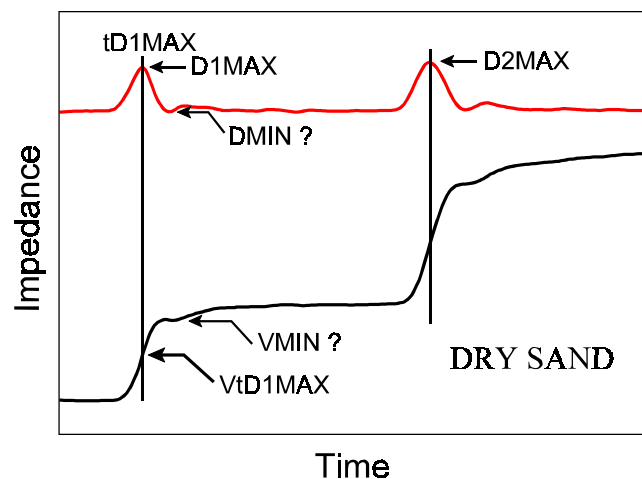


Figure 5. Influence of dry soil on waveform shape illustrating difficulty of finding $DMIN$ and V_{MIN} . The upper line is the first derivative of the waveform.

Another phenomenon sometimes found in low bulk density soils is a double peak in the waveform. This may be due to compression of a thin layer of soil next to the handle as the probe is inserted into the soil at installation time. This higher bulk density soil will exhibit a lower impedance due to lower porosity and correspondingly higher water content (at equilibrium with surrounding soil), thus causing the dip in the waveform after the handle (Air has a permittivity of 1, soil minerals have permittivities of 3 to 5, so denser soils have higher apparent permittivities). As the pulse enters less compressed soil it encounters a higher impedance and the reflected waveform rises, only to lower again as the pulse travels further down the rods (due to the impedance decline associated with the lowering of total resistance with rod length). It is important to have an algorithm to discriminate between these peaks.

INFLUENCE OF BULK ELECTRICAL CONDUCTIVITY ON WAVEFORM SHAPE

As the bulk electrical conductivity (BEC) of the soil increases, the impedance of the waveguide in the soil decreases due to the reduction in the resistive component of impedance. In addition, there is a reduction of signal voltage along the length of the rods due to conduction through the soil. These effects cause the waveform level after the first peak to decline relative to that for a soil of lower BEC. The effects also reduce the slope, D2MAX, of the second rising limb (Hook and Livingston, 1995) and the final height to which the waveform rises after the second inflection (Fig. 6). The latter has been used successfully to find the BEC of soils (e.g. Dalton et al., 1984; Topp et al., 1988; Wraith, 1993).

However, the reduction of D2MAX can make it difficult to find the second rising limb by searching for D2MAX. Smoothing the waveform and its first derivative can make determination of D2MAX more reliable by reducing the relative height of peaks in the first derivative caused by random noise in the waveform. However, in the case of a very weak second rising limb, the peak in the first derivative can be so spread out that the apparent position of the second rising limb, deduced from the position of D2MAX, is not consistent (Fig. 6). Fortunately, in these cases the high BEC guarantees that the waveform will slope downward between t_1 and t_2 , guaranteeing that the position of VMIN is always just before the second rising limb. In this situation, VMIN can be used reliably as the key to an algorithm used to find t_2 (described below).

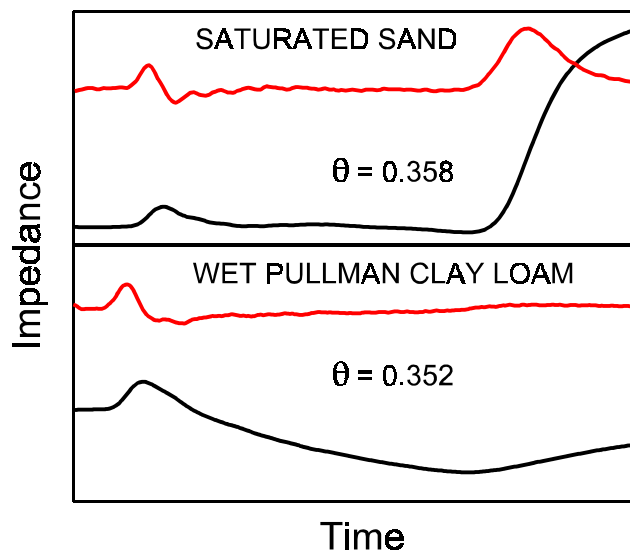


Figure 6. Waveforms and their first derivatives (top line in each plot) for two soils. For the wet clay loam, there is no distinct peak in the first derivative corresponding to the second rising limb of the waveform. But, the position of the lowest part of the waveform, VMIN, occurs just before the second rising limb and may be used to help find t_2 . Although the sand is slightly wetter (θ , $\text{m}^3 \text{m}^{-3}$), there is a distinct peak in the derivative useful for finding t_2 .

Unfortunately, increased soil salinity is only one source of increase in BEC. Another source of BEC is the conductivity arising from certain clays, especially clays with high CEC. These are often expanding lattice clays containing cations entrapped between clay layers. When such soils are dry they exhibit low BEC, probably due to low mobility of cations resulting from the contracted nature of the clay micelles and the discontinuous water films on soil particles. As these soils wet, their BEC increases as shown in Fig. 6 for an expansive Pullman clay loam with mixed mineralogy at Bushland, TX. Effects are apparent as a lowering of the second inflection and final waveform height as these soils wet. Although problems posed by this phenomenon, vis-a-vis the determination of t_2 , can usually be solved, the implications for relating TDR waveforms to soil salinity cannot be ignored.

Furthermore, the reduced slope of the second rising limb has implications for the application of frequency domain (FD) probes to water content determination in these soils, similar to the implications and reported problems related to salinity effects on water content determination by FD probes (Baumhardt et al., 2000). A frequency domain probe relies upon the change in frequency of an oscillator circuit caused by the change in permittivity of the soil around the probe. For the oscillator to change states, the reflected voltage must reach the set point voltage of the oscillator at which time the oscillator changes states and drives the

waveguide to the opposite polarity. To make an analogy between an FD probe and a TDR probe, the time required for the reflected voltage to reach the set point is determined not only by the travel time to t_2 but by the additional time between t_2 and the time at which the second rising limb rises to the set point. Thus, the frequency of oscillation is dependent not only on t_2 or t_2-t_1 but on the BEC of the medium. Because the BEC may be changed by salinity changes, clay content changes, and/or water content changes in a clayey or saline soil it is clear that calibration of an FD probe for routine field use, where these factors may change in time and space, is problematic.

Figure 7 illustrates the general lowering of the reflected step voltage (and thus the increase in apparent BEC) as water content increases for the Pullman soil. Not all clay soils show increases in BEC with water content as shown in Fig. 8 for a Cecil clay of kaolinitic mineralogy from Watkinsville, GA. Figures 7 and 8 illustrate the loss of the first descending limb and VMIN as the soil dries.

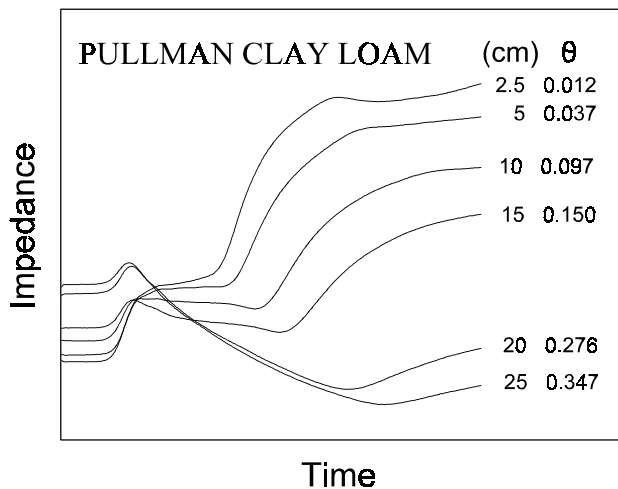


Figure 7. Waveforms from a non-saline Pullman silty clay loam. The effect of soil water content (θ , $\text{m}^3 \text{m}^{-3}$) on the bulk electrical conductivity is large at several depths (cm) in the silty clay loam A horizon (2.5 to 15 cm) and the clay B horizon (20 and 25 cm).

INFLUENCE OF CABLE LENGTH ON WAVEFORM SHAPE

As the pulse moves down the cable to the probe, its higher frequency components are selectively attenuated because the cable acts as a low pass filter. This means that a longer cable causes a slower rise time of the pulse at the probe, and less steep rising and descending limbs of the inflections caused by probe handle and end of rods (Hook et al., 1992; Hook and Livingston, 1995). If the waveform is correctly interpreted, then the travel time, t_r , should be constant despite cable length. However, if the probe is short enough, the descending

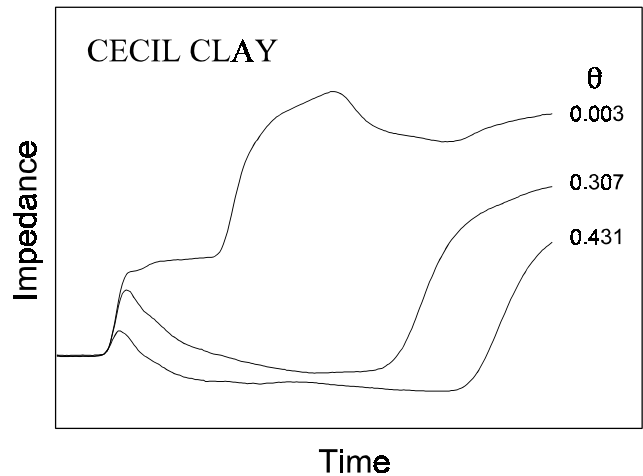


Figure 8. Waveforms from a non-saline Cecil clay (kaolinitic). The effect of soil water content (θ , $\text{m}^3 \text{m}^{-3}$) on the bulk electrical conductivity is small.

limb of the first peak will intersect the rising limb of the second inflection, causing the travel time to be incorrect. A longer cable causes a lower slope of the descending limb, requiring a longer probe to avoid this problem. Since the slope of the descending limb also decreases with increasing BEC of the soil, a probe length adequate for a given cable length is difficult to predict. Another problem associated with long cable lengths is loss of the first peak altogether.

ALGORITHMS FOR WAVEFORM INTERPRETATION

This section describes algorithms used by TACQ for automatic graphical interpretation of a wide variety of waveforms, and discusses errors that may occur with some published methods. The user may choose from several methods described in the literature or use methods available only in TACQ. These methods assume waveforms are correctly positioned in the instrument window as described in Evett (2000). Features of the waveform and its first derivative, discussed below, are defined in Figures 1, 4, and 5. Pre-defined, recommended values of all user choices are stored in TACQ. A detailed list of the steps used in TACQ to interpret waveforms is given in Evett (1999).

WAVEFORM SMOOTHING

Waveforms typically include noise, which when severe can affect the interpretation. Following the method of Baker and Allmaras (1990), waveforms are smoothed using the Savitsky-Golay procedure (Gorry, 1990). The user may choose any degree of smoothing

from none to a 21-point smooth. To provide a symmetrical smooth, only odd numbers of points are allowed. For example, for a 21-point smooth, ten data points before and ten points after each smoothed data point are included. Points nearest the smoothed point contribute most to the smoothing process. The Savitsky-Golay procedure adjusts smoothing coefficients to smooth points at the beginning and end of the waveform where there otherwise would not be enough points. Derivative smoothing may vary from none to a 19-point smooth. Derivative smoothing must be over a number of points at least two lower than the number chosen for waveform smoothing. The user should specify only enough smoothing to reduce extraneous peaks in the first derivative. Excessive smoothing can cause errors, most particularly loss of sharp waveform features such as the first peak. The default setting for smoothing is 9 points on the waveform and 3 points on the first derivative.

CIRCUMSCRIBING WAVEFORM INTERPRETATION

In order to avoid dealing with sudden drops or rises in level that may occur at the beginning or end of the waveform (usually only seen with the older analog Tektronix² model 1502 cable tester), the user may exclude any number of points from waveform interpretation at either end of the waveform. Vertical lines on the screen show the excluded parts of the waveform. The number of excluded points for either end may be set by entering a number or by moving the lines interactively using the cursor keys.

Also, the user may exclude data in the right hand side of the waveform from being used to find the first peaks in the waveform and first derivative. This excludes the second peak in the first derivative from consideration for finding Time 1 and eliminates confusion between the first and second rising limbs. Correspondingly, the user may exclude a portion of the left hand side of the waveform from consideration when determining the location of the second rising limb. Again, these limits may be set by entering a number or by using the cursor keys to move the vertical lines that represent the limits on the computer screen.

CHOOSING WAVEFORM INTERPRETATION METHODS

Time 1. Time 1, t_1 , is defined as the time at which the step pulse exits the probe handle and begins moving down the exposed probe rods (Fig. 1). For finding t_1 ,

the user may choose between two methods. Method M1 is similar to the peak search of Baker and Allmaras (1990), and searches for the peak voltage V_{1MAX} and the subsequent minimum in the first derivative $DMIN$ (Fig. 4). But, it starts the search from the time of the first peak in the first derivative, $D1MAX$ (Fig. 5). A line tangent to the first descending limb of the waveform is drawn at voltage level V_{tDMIN} and time t_{DMIN} , and with slope $DMIN$ (defined in Fig. 4). A horizontal line is drawn across the peak at level V_{1MAX} . The intersection of these lines defines t_1 (Fig. 2), which is the time at which the step pulse exits the probe handle (Fig. 1). If V_{1MAX} and $DMIN$ cannot be found, as might be the case for a dry soil (Fig. 5), the program then uses method M2. Method M2 finds the first peak in the first derivative $D1MAX$ and the corresponding time t_{D1MAX} and waveform level V_{tD1MAX} (Fig. 5). It fits a line tangent to the first rising limb at time t_{D1MAX} and voltage level V_{tD1MAX} . It also fits a horizontal line tangent to the baseline before the first rising limb and then solves the intersection of these lines for $t_{1.bis}$ (Fig. 2). Time $t_{1.bis}$ represents the point in the probe handle where the coaxial cable braid is separated from the inner conductor to connect to the probe rod(s). Method M2 then adds a user-set handle transit time, t_c , to $t_{1.bis}$ to obtain t_1 . The time $t_c = t_1 - t_{1.bis}$ is found by measurements on probes installed in wet soil using both methods M1 and M2, and represents the time necessary for the step pulse to travel within the handle from the point of separation of the coaxial cable braid to the point where the probe rods exit the handle. For the trifilar probes developed by the author (model TR-100, Dynamax, Houston, TX), t_c equals 0.52 ns. Method M2 is the default method for Time 1.

Method M2 is different from that proposed by Heimovaara and Bouten (1990) involving a single measurement in air that supplied the travel time to the probe handle. This travel time, $t_{1.bis}$, was then used for all future measurements. By contrast, TACQ measures $t_{1.bis}$ every time a waveform is interpreted. The reason for this is that the pulse travel time to the handle varies as the temperature of the intervening cable changes, and the variation in the value of $t_{1.bis}$ can introduce considerable error in the calculated probe travel time, t_p , and water content. For example, data from 72 probes in a field experiment showed that $t_{1.bis}$ varied diurnally, with a mean range of 0.1 ns (SD = 0.03 ns) over an 86 day period. For the 20 cm probes used, the relationship between water content, θ ($m^3 m^{-3}$), and travel time, t_p (ns), is $\theta = -0.19 + 0.090(t_p)$, and the error induced by the varying value of $t_{1.bis}$ is on the order of

² The mention of trade or manufacturer names is made for information only and does not imply an endorsement, recommendation, or exclusion by USDA-Agricultural Research Service.

$0.01 \text{ m}^3 \text{ m}^{-3}$. For five of the probes, the variation in $t1.bis$ over the period approached 0.28 ns , or an error of $0.026 \text{ m}^3 \text{ m}^{-3}$ (Fig. 9). For a water content measurement method that can achieve precision on the order of $0.0006 \text{ m}^3 \text{ m}^{-3}$ (Evelt, 1998) errors of this size are not acceptable. If change in stored moisture were measured over the 86 day period, the decrease in $t1.bis$ would result in an increase in measured water content change of $0.026 \text{ m}^3 \text{ m}^{-3}$. For probes shorter than 20 cm, the error in water content induced by not determining $t1.bis$

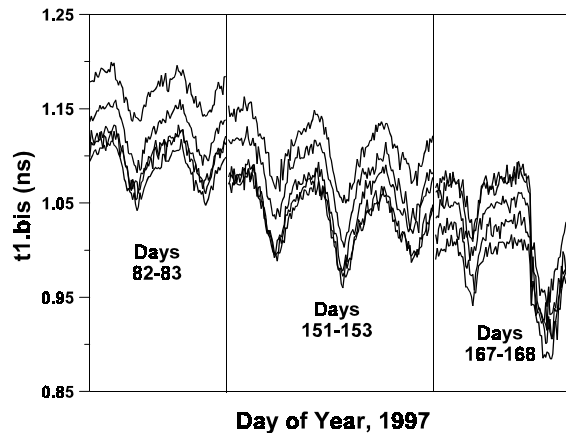


Figure 9. Variation of $t1.bis$ over an 86 day period in 1997 for five probes in a field experiment at Bushland, Texas. The value of $t1.bis$ decreased as temperature increased, both diurnally and over the period. This was probably due to temperature affecting the permittivity of the coaxial cable insulation. Other experiments, in which the TDR cable tester was kept in an isothermal environment (within 1°C) showed similar effects of temperature, indicating that variations in cable temperature are the cause for variations in $t1.bis$.

for every waveform would be even larger.

Time 2. Time 2, $t2$, is defined as the time at which the step pulse reaches the distal ends of the probe rods (Fig. 2) where it is reflected back, causing the second rising limb of the waveform (Fig. 1). It often may be found from the intersection of a line, drawn tangent to the steepest part of the second rising limb of the waveform, and a horizontal line drawn tangent to the “global minimum” of the waveform as defined in Fig. 1. The steepest part of the rising waveform is identified by finding the second peak in the first derivative. However, as mentioned above, in some wet soils the second peak in the first derivative can be difficult to find; and in very dry soil the “global minimum” can be difficult to find. Thus, alternative strategies are used by the program, which will automatically switch between these strategies to find the best interpretation of Time 2 as follows:

Tangent to Rising limb. For finding the center of the second rising limb (time $t2.2$ in Fig. 4), the user

may choose one of three methods. Method 1 finds the second peak in the first derivative $D2MAX$ and associated time $t2.2$ (Fig. 4). Method 2 finds $VMIN$ and $t2.1$ (Fig. 4) and sets $t2.2$ as $t2.1$ plus a user-set number of points. Method 3 is an automatic method that uses method 1 if the value of $D2MAX$ is above a user-set threshold, $D2Thresh$, and that uses method 2 otherwise. The default value of $D2Thresh$ in TACQ is for a waveform from a Tektronix 1502B/C cable tester captured at 13 bit resolution and no gain. Method 3 is recommended. It will find the center of the rising limb from the position of $VMIN$ if the value of $D2MAX$ is so low that the position of $D2MAX$ is uncertain (e.g. lower part of Fig. 6); and it will use the position of $D2MAX$ otherwise. Method 3 relies on the fact that, when $D2MAX$ is low, the position of $VMIN$ is always easily identified and always occurs just before the second rising limb. Method 1 is similar to that of Baker and Allmaras (1990), except that the search for $VMIN$ is conducted in the data after time $t1$ rather than over all the data. Regardless of the method for finding $t2.2$, the line tangent to the second rising limb is found by linear regression on a swath of points around $t2.2$ (user chosen swath width).

Tangent to $VMIN$ or Fit to Base Line. The user may use one of two methods to fit the “horizontal” intersecting line that partially defines $t2$. Method 1 is a horizontal line passing through the waveform at level $VMIN$. Method 2 is a line fit by regression to a swath of points just prior to $t2.1$ (e.g., Fig. 2) (user-chosen swath width and position). Method 2 is recommended. Travel times found with it are less susceptible to temperature induced errors (Wraith and Or, 1999), and may be less susceptible to errors due to clay mineralogy and soil bulk electrical conductivity. If the horizontal tangent method is chosen, the program will also use method 2, and if the slope of a line fitted to the swath of points is positive, the program will use the fitted line rather than the horizontal tangent. This avoids improper interpretation of waveforms from dry soils for which $VMIN$ may be located closer to $t1$ than $t2$ and the waveform slope may be positive between $t1$ and $t2$.

Screen shots from TACQ illustrate some of these Time 2 interpretation procedures. In Figure 10A, we see a waveform acquired from a wet soil. The automatic method for determining Time 2 was invoked and the value of $D2MAX$ was lower than $D2THRESH$, causing the position of $VMIN$ ($t2.1$) to be used as a starting point. The center of the rising limb at $t2.2$ was found by adding a user-set number of points to the position of $VMIN$; and a line tangent to the rising limb was found by linear regression on a swath of points around $t2.2$

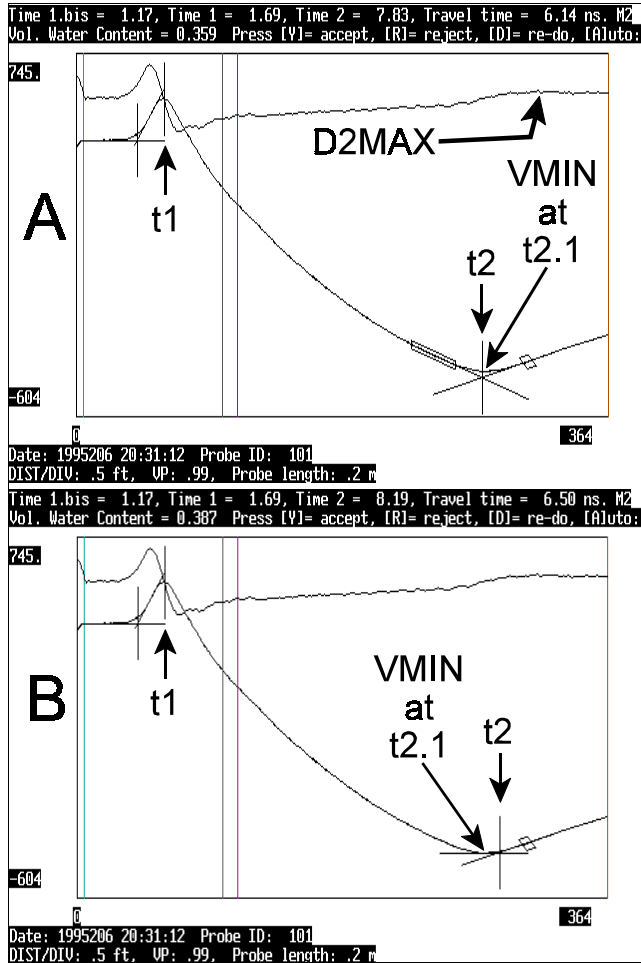


Figure 10. Two screen shots from TACQ.EXE showing alternative interpretation methods for Time 2. In A, the position of VMIN is used to find the center of the rising limb by moving to the right 40 points. The box around the rising limb shows the swath of points to which a tangent line was fit by linear regression. The box around the waveform to the left of VMIN shows the swath of points to which the second tangent line was fit. In B, the second tangent line is simply a horizontal line at VMIN. Data are from a Tektronix 1502 cable tester digitized at 364 points across the window and connected to a 20-cm trifilar probe in wet Pullman clay loam.

shown by the box around the waveform to the right of t_2 . The tangent to the waveform prior to $t_{2.1}$ (before VMIN) was found by linear regression on a swath of points that ended at 0.8 of the distance between Time 1 and $t_{2.2}$. The user can set both the number of points in the swath and the ending point of the swath as a fraction of the time between Time 1 and $t_{2.2}$. The program contains default values for all user-settings that work well for waveforms captured from Tektronix 1502B/C cable testers using the window width settings discussed in Evett (2000). Figure 10B shows that if method 2 for the base line fit is used then the line is horizontal and passes through VMIN. This causes Time 2 to be increased by 0.36 ns, with a resulting increase of $0.028 \text{ m}^3 \text{ m}^{-3}$ in water content reported.

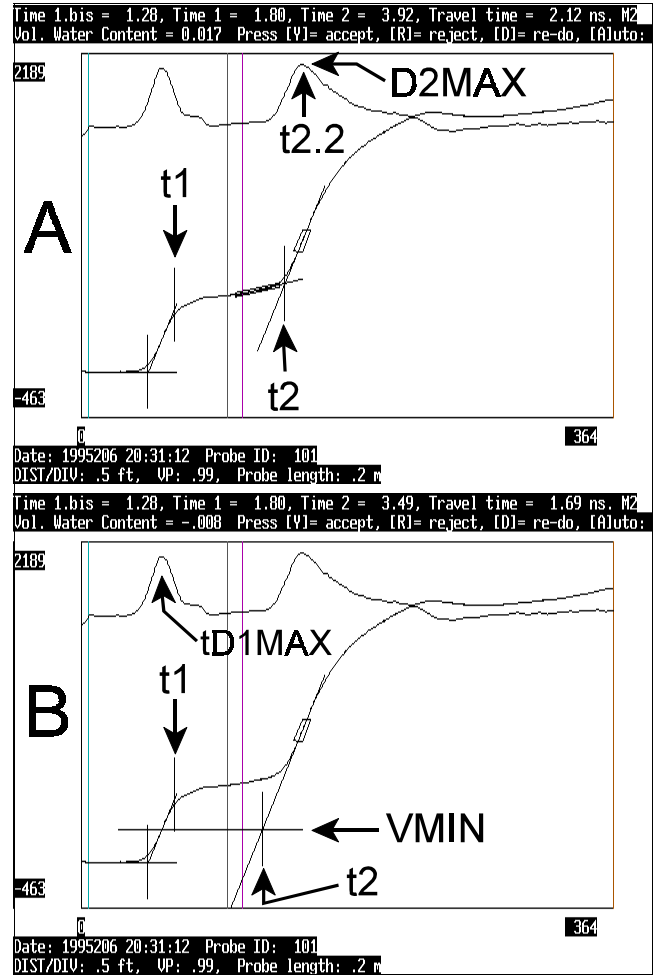


Figure 11. Two screen shots from TACQ.EXE showing alternative interpretation methods for Time 2 in a dry Pullman clay loam. In A, The time of the second peak in the first derivative, D2MAX, is well defined and is used to define the center of the second rising limb of the waveform at $t_{2.2}$. A tangent line is fit to a swath of waveform data points around $t_{2.2}$ as shown by the box and line there. A second tangent line is fit to a swath of points that ends at 0.8 of the time between t_1 and $t_{2.2}$. The intersection of these lines defines t_2 . In B, the search for the lowest point between t_1 and the end of the waveform resulted in finding VMIN at t_{D1MAX} , the time of the first peak in the first derivative. A horizontal line drawn at this point clearly results in incorrect interpretation.

In Figure 11A, the waveform is from the same probe, but when the soil was dry. The value of D2MAX was high enough that the time of D2MAX ($t_{2.2}$) was well defined. The tangent to the rising limb was found by linear regression on a swath of points around $t_{2.2}$. The line tangent to the waveform prior to the second rising limb was found by linear regression on a swath of points that ended at 0.8 of the distance between Time 1 and $t_{2.2}$. Figure 11B shows the $-0.025 \text{ m}^3 \text{ m}^{-3}$ error in water content that occurs when the base line fit prior to the second rising limb is made by drawing a horizontal line across VMIN, which cannot be found in its usual

position because the waveform rises continuously in this very dry soil.

SUMMARY AND DISCUSSION

The TACQ computer program was developed to automatically control a stand-alone TDR system consisting of a TDR instrument, up to seventeen multiplexers, and up to 256 probes. Automatic graphical interpretation of waveforms includes methods given in the TDR literature as well as methods unique to TACQ that allow the program to correctly interpret waveforms from many different soils. Soils used in the development of TACQ include the Amarillo fine sandy loam (fine-loamy, mixed, superactive, thermic Aridic Paleustalf), Cecil clay (fine, kaolinitic, thermic Typic Kanhapludult), Olton clay loam (fine, mixed, superactive, thermic Aridic Paleustoll), Pullman clay loam (fine, mixed, superactive, thermic Torrertic Paleustoll), Ulysses silt loam (fine-silty, mixed, superactive, mesic Aridic Haplustoll), an unclassified coarse desert sand in Ismailia, Egypt, and commercial silica sands. The user has complete control over the interpretation methods used, the acquisition interval, the kind of data acquired for each probe, and the interconnection of probes and multiplexers. Data for water content, bulk electrical conductivity, and temperature measurements may be collected.

Published methods for determining Time 2 can cause errors as illustrated in Figures 10 and 11. If these errors were to occur in an experiment designed to determine change in storage of a soil profile as a crop extracted water, the result could be an increased value of change in stored water approaching $0.053 \text{ m}^3 \text{ m}^{-3}$. Errors in the determination of Time 1 can arise from some published methods, and can cause an apparent increase in water content as large as $0.026 \text{ m}^3 \text{ m}^{-3}$ as temperature increases over a growing season, or as large as $0.01 \text{ m}^3 \text{ m}^{-3}$ during a day under our conditions (Fig. 9). Discrepancies this large could easily account for some of the reported TDR calibration studies that were at odds with the results of Topp et al. (1980). Because interpretation methods can have a large effect on reported water contents, these methods should be reported in calibration studies and other TDR methodology studies. The default methods in TACQ avoid the illustrated errors in waveform interpretation for soils of widely varying water content, texture, mineralogy, and bulk density.

ACKNOWLEDGMENTS. This work has benefited from discussions with John Baker, Jon Wraith, Egbert Spaans, Dani Or, Jim Simpson, Clark Topp, Mike Young, and many others. Nevertheless, any errors are my own. The Cecil clay soil was provided by Jean Steiner, Director, USDA-ARS, J. Phil Campbell, Senior Natural Resource Conservation Center, Watkinsville, GA.

REFERENCES

- Baker, J.M., and R.R. Allmaras. 1990. System for automating and multiplexing soil moisture measurement by time-domain reflectometry. *Soil. Sci. Soc. Am. J.* 54(1):1-6.
- Dalton, F.N., W.N. Herkelrath, D.S. Rawlins, and J.D. Rhoades. 1984. Time-domain reflectometry: simultaneous measurement of soil water content and electrical conductivity with a single probe. *Science* 224: 989-990.
- Baumhardt, R.L., R.J. Lascano, and S.R. Evett. 2000. Soil material, temperature, and salinity effects on calibration of multisensor capacitance probes. *Soil Sci. Soc. Amer. J.* Nov.-Dec. 2000.
- Evett, S.R. 1993. Evapotranspiration by soil water balance using TDR and neutron scattering. In *Management of Irrigation and Drainage Systems*, Irrigation and Drainage Div./ASCE, July 21-23, 1993, Park City, Utah. pp. 914-921.
- Evett, S.R. 1994. TDR-Temperature arrays for analysis of field soil thermal properties. Pp. 320-327 *In* Proceedings of the Symposium on Time Domain Reflectometry in Environmental, Infrastructure and Mining Applications, Sept. 7-9, 1994. Northwestern University, Evanston, Illinois. USDI, Bureau of Mines, Special Publication SP 19-94.
- Evett, S.R. 1998. Coaxial multiplexer for time domain reflectometry measurement of soil water content and bulk electrical conductivity. *Trans. ASAE* 42(2):361-369.
- Evett, S.R. 2000a. Some Aspects of Time Domain Reflectometry (TDR), Neutron Scattering, and Capacitance Methods of Soil Water Content Measurement. Pp. 5-49 *In* Comparison of soil water measurement using the neutron scattering, time domain reflectometry and capacitance methods. International Atomic Energy Agency, Vienna, Austria, IAEA-TECDOC-1137.
- Evett, S.R. 2000b. The TACQ Computer Program for Automatic Time Domain Reflectometry Measurements: I. Design and Operating Characteristics. *Trans. ASAE* 43(6):1939-1946.
- Gorry, P.A. 1990. General least-squares smoothing and differentiation by the convolution (Savitsky-Golay) method. *Anal. Chem.* 62:570-573.

- Heimovaara, T.J. 1993. Design of triple-wire time domain reflectometry probes in practice and theory. *Soil Sci. Soc. Am. J.* 57:1410-1417.
- Heimovaara, T.J., and W. Bouten. 1990. A computer-controlled 36-channel time domain reflectometry system for monitoring soil water contents. *Water Resour. Res.* 26(10):2311-2316.
- Herkelrath, W.N., S.P. Hamburg, and F. Murphy. 1991. Automatic, real-time monitoring of soil moisture in a remote field area with time domain reflectometry. *Water Resour. Res.* 27(5):857-864.
- Hook, W.R., N.J. Livingston, Z.J. Sun, and P.B. Hook. 1992. Remote diode shorting improves measurement of soil water by time domain reflectometry. *Soil Sci. Soc. Am. J.* 56:1384-1391.
- Hook, W.R., and N.J. Livingston. 1995. Propagation velocity errors in time domain reflectometry measurements of soil water. *Soil Sci. Soc. Am. J.* 59:92-96.
- Savitsky, A., and M.J.E. Golay. 1964. Smoothing and differentiation of data by simplified least squares. *Anal. Chem.* 36:1627-1639.
- Spaans, E.J.A., and J.M. Baker. 1993. Simple baluns in parallel probes for time domain reflectometry. *Soil Sci. Soc. Am. J.* 57:668-673.
- Topp, G.C., J.L. Davis, and A.P. Annan. 1980. Electromagnetic determination of soil water content: Measurements in coaxial transmission lines. *Water Resour. Res.* 16(3):574-582.
- Topp, G.C., J.L. Davis, and A.P. Annan. 1982. Electromagnetic determination of soil water content using TDR: I. applications to wetting fronts and steep gradients. *Soil Sci. Soc. Am. J.* 46:672-678.
- Topp, G.C., M. Yanuka, W.D. Zebchuk, and S. Zegelin. 1988. Determination of electrical conductivity using time domain reflectometry: Soil and water experiments in coaxial lines. *Water Resour. Res.* 24:945-952.
- Williams, T. 1991. *The Circuit Designer's Companion*. Butterworth-Heinemann, Ltd., Pub. 302 pp.
- Wraith, J.M., S.D. Comfort, B.L. Woodbury, and W.P. Inskeep. 1993. A simplified waveform analysis approach for monitoring solute transport using time-domain reflectometry. *Soil Sci. Soc. Am. J.* 57:637-642.
- Wraith, J.M., and D. Or. 1999. Temperature effects on soil bulk dielectric permittivity measured by time domain reflectometry: Experimental evidence and hypothesis development. *Water Resour. Res.* 35(2):361-369.
- Zegelin, S.J., I. White, and D.R. Jenkins. 1989. Improved field probes for soil water content and electrical conductivity measurement using time domain reflectometry. *Water Resour. Res.* 25(11):2367-2376.